Research Paper

Correlation between Urban Density and Heat Health Risk in Megacities: A Case Study of Shenzhen

Cunyan JIANG, School of Architecture, Harbin Institute of Technology, China

Zide LIU, School of Architecture, Harbin Institute of Technology, China

Abstract

Global climate change has led to more frequent extreme heat events, while the urban heat island effect exacerbates heat health risk in densely populated cities. Shenzhen, one of China's fastest-growing cities, has undergone rapid urban expansion over the past two decades, resulting in significant challenges related to heat health risk. Balancing accelerated urbanization with sustainable design principles is crucial for developing livable and resilient urban environments. This study aims to elucidate the correlation between building density and the deterioration of the urban thermal environment in megacities by Geographically Weighted Regression Models and to propose planning and policy measures aligned with sustainable design to mitigate heat health risk in high-density urban areas. The results indicate (1) a significant spatial autocorrelation of heat health risk and (2) a significant positive correlation between building density and heat health risk. These findings underscore the importance of urban planning in alleviating heat health risk through the reduction of building density. Using Shenzhen as a case study, this research examines the impact of megacity construction on thermal environment degradation and increased heat health risk and discusses sustainable planning and policy interventions to reduce these risks, offering recommendations for creating livable and resilient cities.

Keywords

Heat health risk, Megacities,Building density, Geographically Weighted Regression Models

1. Introduction

As global climate change intensifies, the intensity, duration, and frequency of extreme heat events will continue to increase, posing a serious threat to human health. The Sixth Assessment Report (AR6) of the United Nations Intergovernmental Panel on Climate Change (IPCC) shows that "Global surface temperature was about 1.1°C above 1850-1900 in 2011-2020 (1.09 [0.95 to 1.20]°C), with larger increases over land (1.59 [1.34 to 1.83]°C) than over the ocean (0.88 [0.68 to 1.01]°C)(Intergovernmental Panel on Climate Change, 2021). Lei Zhao et al. (2021) found by modeling climate projections that many of the world's cities could warm by as much as 4°C if greenhouse gas emissions continue at high levels through 2100. Extreme hot weather overwhelms the human thermoregulatory system, which can lead to heat stroke for residents, significantly the frail, such as children and the elderly, and if not treated in time, can aggravate severe illnesses such as pyrexia, which can then lead to vital organ failure or even death (Yuan et al., 2021).

Due to urbanization, the urban heat island (UHI) effect has become a modern endemic threat to human health and energy consumption, especially in compact urban areas with high population density (Lin et al., 2017). High-density cities have been shown to have a stronger heat island effect (Hien, Jusuf and Jiang, 2019). Cities consist of urban form patterns with different building characteristics and have specific microclimatic characteristics (Chen et al., 2021). In dense urban areas, an increase in building density leads to an increase in surface temperature (Sun, 2020). Shenzhen is one of the most densely populated cities in the world and is also prone to extreme heat events. Therefore, it has become imperative to accurately assess the impact of heat health risk in high-density cities and to propose targeted adaptation strategies and mitigation measures.

Currently, urban thermal environment research mainly focuses on high-temperature risk assessment, the impact mechanism of UHI effect, and risk response strategies (Liu, Chen & Wang 2022). In studies related to urban heat health risk assessment, the indicators employed to reflect the elements of health heat risk are not comprehensive enough to fully express the attributes of the elements. Furthermore, the correlation between building density and heat health risk has not received the attention it warrants. To address the limitations of heat health risk-related studies, this research analyzes multivariate data, such as remote sensing images, to obtain more relevant indicators to construct a more detailed heat health risk assessment. It introduces Geographically Weighted Regression (GWR) analysis to explore the correlation between building density and heat health risk in the spatial dimension to more accurately capture the changing patterns of variables and the extent.

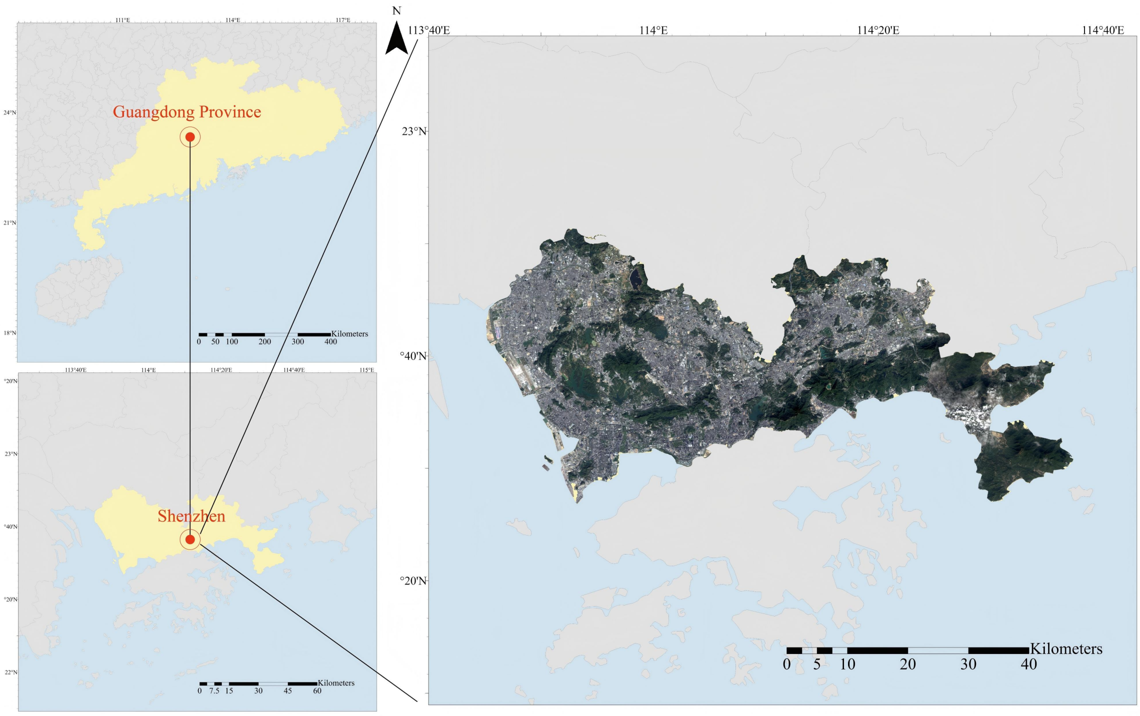

Figure 1. The geographic location of Shenzhen, China.

2. Study area

Shenzhen (22°27′-22°52′N, 113°46′-114°37′E) is located on the southeast coast of China and is a very representative megacity in the Guangdong-Hong Kong-Macau Greater Bay Area(Fig. 1). Since the 21st century, Shenzhen has experienced rapid urbanization, and large-scale urban construction has led to significant changes in spatial structure and surface materials, resulting in increasingly pronounced high temperatures, with a historical extreme maximum temperature of 38.7°C (Zhao et al., 2021). Identifying and assessing heat health risk and proposing related strategies to make Shenzhen a more livable and resilient city has become an important goal for future urban planning in Shenzhen.The scope of this paper is the whole city of Shenzhen, including Futian District, Luohu District, Yantian District, Nanshan District, Bao'an District, Longgang District, Longhua District, Pingshan District, Guangming District and Dapeng New District. It has a total area of 1,997.47 square kilometers and a permanent population of 17.7901 million.

3. Methodology

The heat health risk assessment model, which is based on the Crichton's risk triangle framework as outlined in the IPCC Fifth Assessment Report, has been widely recognized and applied in academic and professional circles (Hu et al., 2017). In this study, the framework is employed to calculate the components of heat health risk, including heat hazard, heat exposure, and heat vulnerability. The heat health risk index of Shenzhen is obtained through the weighted multiplication of these three factors. This study utilizes methods such as spatial autocorrelation analysis and geographically weighted regression analysis to analyze the correlation between building density and heat health risk, and proposes targeted strategies to mitigate heat health risk based on the results. Fig. 2 illustrates the study flow.

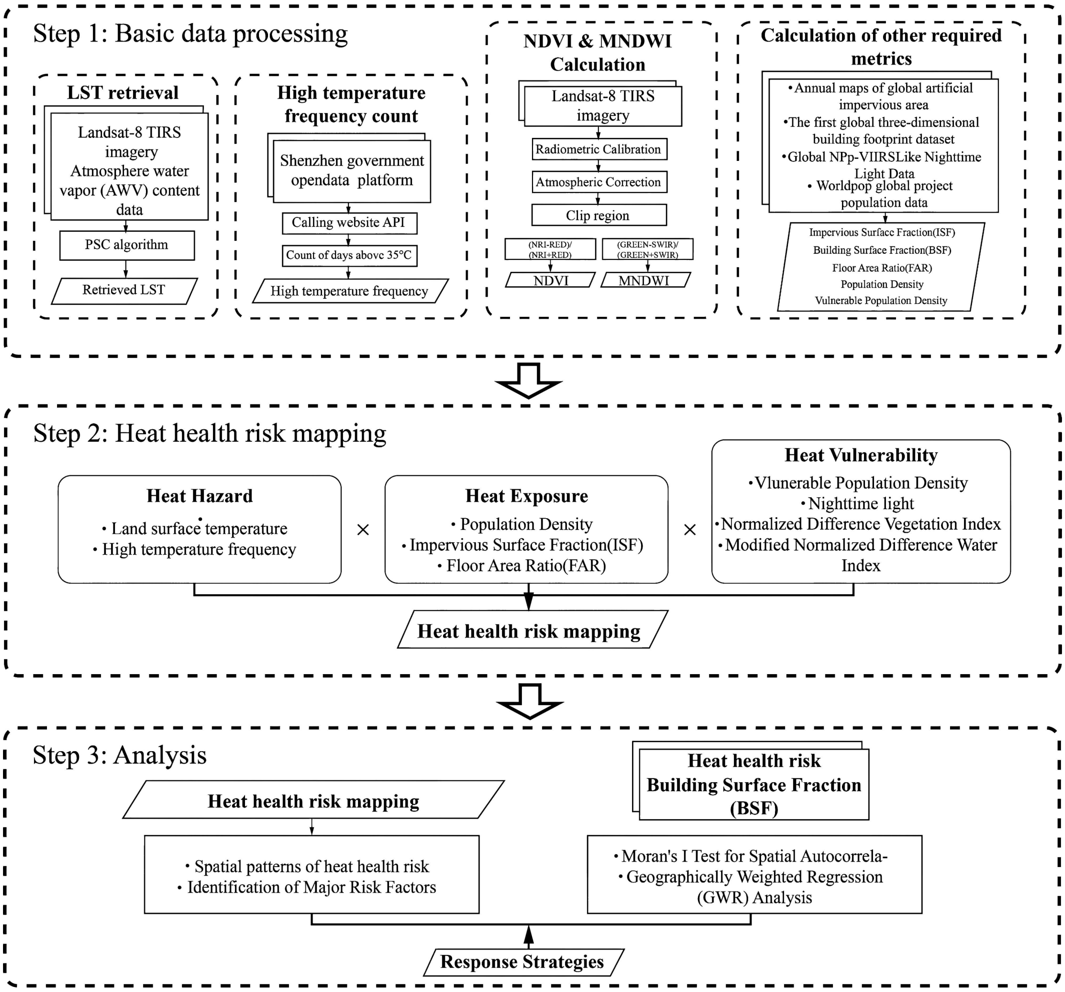

Figure 2. The workflow for this study.

3.1. Data collection and preprocessing

This study mainly collected Landsat 8 remote sensing image data, built environment data (including impervious surface data and building vector data), Shenzhen meteorological data, and socioeconomic data (including worldpop population density data and nighttime light data) to calculate the components of heat health risk and building density in Shenzhen. The specific sources and applications of each data are shown in Table 1. Considering the resolution of different data, a 300m grid was used as the research unit for data processing, which can well reflect the heterogeneity of urban areas and ensure the macro-control of urban planning.

Table 1. Summarized information of datasets used in this study.

Theme	Sources	Period	Resolution	Application
Landsat-8	Geospatial Data Gloud (https://www.gscloud.cn/)	2021.12.5 and 2021.12.14	30m	NDVI/MNDWI calculation
Impervious surface data	Urban Environmental Monitoring and Modeling (UEMM) team(Gong et al., 2020)	2021	30m	ISF calculation
Building vector data	Zenodo database by Che et al. (2024)	2020	-	Building density and floor area ratio calculation
Meteorological data	Shenzhen Municipal Government Data Open Platform (https://opendata.sz.gov.cn/data/dataSet/toDataDetails/)	2021	-	Hazard calculation
Population density data	WorldPop(https://www.worldpop.org/)(WorldPop, 2018a; WorldPop, 2018b; Nieves et al., 2020a; Nieves et al., 2020b; Pezzulo et al., 2017)	2020	100m	Exposure/ Vulnerability calculation
Nighttime light data	An extended time-series (2000-2023) of global NPP-VIIRS-like nighttime light data by Chen Zuoqi et al. (2021)	2020	500m	Vulnerability calculation

3.2. Framework for heat health risk assessment

Heat health risk assessment is the foundation and research focus of urban heat health risk management. In 2014, the fifth assessment report of the IPCC elucidated the concept and evaluation methodology of climate change risk, indicating that such risk arises from the interaction between climate hazards and human and natural systems, and it is determined by the hazard of the disaster, the exposure, and the vulnerability of the disaster-bearing body (Field et al., 2014). This study will quantify and estimate heat health risk using IPCC-endorsed Crichton's Risk Triangle approach. The indicators will be chosen after a literature study and data availability evaluation.

The heat health risk is calculated through the weighted integration of three indices: heat hazard, heat exposure, and heat vulnerability. Due to the lack of uniformity in the weights of these indices (Johnson et al., 2012), this study employs an equal-weight multiplication and division method to compute the heat health risk index, thereby illustrating the intricate relationship among the indices. The formula is shown below:

$$HRI = \text{hazard} \times \text{exposure} \times \text{vulnerability} \tag{1}$$

In order to ensure the comparability between the three elements as above and to achieve aggregation at the level of indicators and components, this study has standardized all indicators to avoid the appearance of zero values. The standardized calculation formulas for positive and negative impact indicators are shown in formulas (2) and (3):

$$V' = 0.1 + \frac{V - Min}{Max - Min} \times (0.9 - 0.1) \tag{2}$$

$$V' = 0.1 + \frac{Max - V}{Max - Min} \times (0.9 - 0.1) \tag{3}$$

Where V' is the normalized value, V is the original value, Max and Min are the maximum and minimum values of the original value, respectively.

3.2.1 Heat Hazard

Heat hazards are the causes and triggers of heat-related calamities and heat health risks. It focuses on high-temperature heat waves, UHI effect, urban anthropogenic heat sources, transportation heat emissions, and urbanization. This study uses LST and heat wave frequency to assess heat threat. According to Shenzhen Meteorological Bureau records and climatic standards, summer in Shenzhen is April 21–November 2.

In this study, we use the PSC method to compute the average LST from April 21 to November 2, 2021, through GEE, and the formula of the PSC method is as follows (Wang et al., 2019):

$$\text{LST} = \frac{c_2}{\lambda \ln\left(\frac{c_1}{\lambda^5 \cdot B(T_S)} + 1\right)} \tag{4}$$

$$B(T_S) = a_0 + a_1\omega + (a_2 + a_3\omega + a_4\omega^2)\frac{1}{\varepsilon} + (a_5 + a_6\omega + a_7\omega^2)\frac{L_{sen}}{\varepsilon} \tag{5}$$

In the formula, LST is the land surface temperature in (K); $B(T_S)$ is the Planck's radiation function based on the temperature T_S; λ is the effective wavelength; L_{sen} is the radiation received by the sensor; ε is the surface albedo; ω is the atmospheric water vapor content; c_1 and c_2 is a constant equal to 1. 19104×108W · μm 4 · m2 · sr-1, 1.43877×10-4 μm · K; the coefficients a_K (K=0,1,2...) are : -0.4107, 1.493577, 0.278271, -1.22502, -0.31067, 1.022016, -0.01969, 0.036001 in Landsat-8.

The higher the heat wave frequency, the higher the heat wave hazard (Anderson and Bell, 2011). According to the definition of hot weather by the China Meteorological Administration, this study was conducted to calculate the heat wave frequency by counting the total number of days with temperatures higher than 35°C in 2021 in each administrative district of Shenzhen (Dong et al., 2014; Hu et al., 2017). The indicators were standardized and then summed with equal weights to calculate the heat hazard index using the following formula:

$$\mathrm{Hazard} = (\mathrm{LST} + \mathrm{F})/2 \tag{6}$$

In the formula, LST is the average land surface temperature of Shenzhen from April 21 to November 2, 2021, and F is the heat wave frequency.

3.2.2 Heat Exposure

Heat exposure is the objective physical environment in cities that enhances heat health risk and may worsen heat catastrophes. Impervious surface ratio (ISF) and floor area ratio (FAR) might indicate inadequate ventilation, cooling, heat radiation, and reflection. Since urban heat health risk research focuses on individuals, population density indicates heat exposure (Buscail, Upegui and Viel, 2012). FAR is the ratio of total floor area to grid area and indicates building density and development intensity. The formula is:

$$\mathrm{FAR} = \frac{\sum_{i=1}^{n} F_i A_{Bi}}{A_P} \tag{7}$$

A_{Bi} is the floor area of the ith building within the grid, F_i is the number of floors of the ith building within the grid, and A_P is the grid area.

ISF reflects the coverage ratio of impervious surfaces within the grid. The calculation formula is:

$$\mathrm{ISF} = 1 - \mathrm{BSF} - \mathrm{PSF} \tag{8}$$

Population density data are obtained from the WorldPop gridded population density dataset (Unconstrained individual countries 2000-2020) with a resolution of 100m. The heat exposure index is calculated by standardizing the FAR, ISF, and population density and then adding them equally, as follows:

$$\mathrm{Exposure} = (\mathrm{FAR} + \mathrm{ISF} + \mathrm{POP})/3 \tag{9}$$

POP is the population density.

3.2.3 Heat Vulnerability

Heat vulnerability is the city's socio-economic circumstances that raise heat health risk, stressing the losses and injuries urban people or institutions may experience in heat disasters. Vulnerable infrastructure systems, poor economic levels, barren vegetation and water bodies, vulnerable populations (elders and children), etc., are typically reflected by indicators like vulnerable population density, nocturnal light index, NDVI, and MNDWI. The formulas are as follows：

$$\mathrm{NDVI} = \frac{\mathrm{NRI} - \mathrm{RED}}{\mathrm{NIR} + \mathrm{RED}} \tag{10}$$

$$\mathrm{MNDWI} = \frac{\mathrm{GREEN} - \mathrm{SWIR}}{\mathrm{GREEN} + \mathrm{SWIR}} \tag{11}$$

NIR is the near infrared band (B5); RED is the red light band (B4); GREEN is the green light band (B3); and SWIR is the shortwave infrared band 1 (B6). Previous studies have shown that nighttime light data can reflect socioeconomic levels. Residents over the age of 65 and under the age of 5 are generally considered to be more vulnerable to high temperatures. Therefore, the density of these vulnerable populations is selected as an indicator of heat vulnerability in the heat health risk assessment. NDVI, MNDWI, and nighttime light Index are higher, the lower the heat vulnerability, so the three are used as negative effect indicators, and the density of vulnerable populations is normalized and then subtracted in equal weight to calculate the Heat Vulnerability Index. The formula is as follows:

$$\text{Vulnerability} = (\text{POP}' - \text{NDVI} - \text{MNDWI} - \text{NL})/4 \quad (12)$$

POP' is the density of vulnerable people, NDVI is the normalized difference vegetation index, MNDWI is the modified normalized difference water index, and NL is the nighttime light index.

3.3. Geographically weighted regression analysis model

3.3.1 Spatial autocorrelation analysis

A variable shows spatial autocorrelation when it shows regularity rather than random distribution in space. Moran (1948) applied the one-dimensional correlation coefficient in two-dimensional space to study random distribution phenomena in two-dimensional space and then proposed Moran's index (Moran, 1950). Moran's index can be used to assess the degree of spatial autocorrelation between variables at adjacent locations.

3.3.2 Geographically weighted regression analysis

Studies have shown that there is spatial non-stationarity in the relationship between LST and its forcing factors (Lu et al., 2021; Liu et al., 2019). For this reason, scientists have introduced the method of geographically weighted regression analysis (Guo et al., 2020; Liu et al., 2021). Geographically weighted regression is a spatial analysis technique proposed by Fotheringham et al. (1998) to deal with spatial heterogeneity (Lu et al., 2020). It can be used to quantify the correlation between variables and their spatial heterogeneity (Li, Zhao and Xu, 2017). In this paper, after verifying the spatial heterogeneity of thermal health risks, a geographically weighted regression model is introduced to further analyse the relationship between building density and thermal health risks.

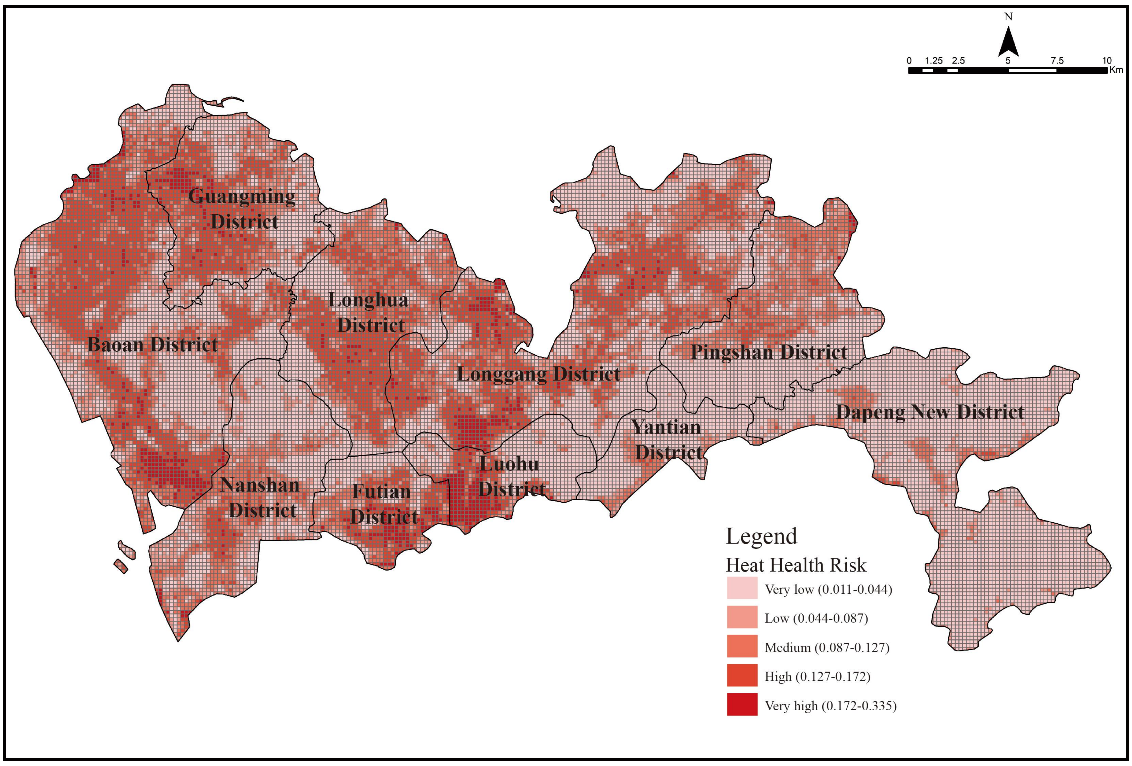

Figure 3. Heat health risk assessment result.

4. Results

4.1. Shenzhen Heat Health Risk Assessment Results

ArcGIS Pro was used to overlay the heat hazard, heat exposure, and heat vulnerability indices to obtain a heat health risk index, which was then classified into five levels: very high, high, medium, low, and very low using the natural breakpoint classification method (Fig. 3).

4.2. A study on the correlation between building density and heat health risk

As can be seen from the above analysis, differences in geographical location may have an impact on heat health risks, leading to spatial heterogeneity in heat health risks. The OLS results (as shown in Table 2 and Table 3) show that building density is significant at the 0.01 level, and the joint F statistic passes the significance test, which model is statistically significant; the probability of the Koenker (BP) statistic is less than 0.01, indicating statistical significance, which indicates that the model is unstable and there may be spatial heterogeneity, so it is necessary to introduce a GWR model for further analysis.

Table 2. OLS Model Estimation.

Variable	P-value
BSF	0.000000**

Table 3. OLS Diagnostic Results（"" indicates statistical significance at the 0.01 level (two-tailed).）.**

Diagnostic	
R2	0.508884
Adjusted R^2	0.508862
Joint Chi-square Statistic	17114.727069**
Joint Chi-square P-value	0.000
Joint F-statistic	23248.718771**
Joint F-statistic P-value	0.000
Akaike Information Criterion (AICc)	-81919.767888
Koenker (BP) Statistic	76.613268**
Koenker (BP) P-value	0.000

4.2.1 Moran's index test

Before conducting a GWR analysis, it is first necessary to check whether there is spatial autocorrelation in heat health risks. The Moran's I index is used to analyze whether the hypothesis of spatial autocorrelation of heat health risks is valid. The results of the Moran's I analysis are shown in Fig. 4. The z-score is as high as 170.787853, which is much higher than the usual significance threshold, indicating that there is a positive correlation. The p-value is 0.000000, which is much smaller than 0.01, meaning that the possibility of the data being randomly distributed is less than 1%, indicating that the heat health risk has spatial agglomeration characteristics within Shenzhen, and the possibility of the results being random can be almost completely ruled out. Therefore, the GWR is introduced in this study for further analysis.

4.2.2 Geographically weighted regression analysis

Moran's I test shows that the heat health risk in Shenzhen has a significant spatial correlation. Traditional regression models cannot incorporate geographical location information, while the GWR model can be used to effectively explore the issue of local heterogeneity between independent variables and dependent variables caused by geographical location.

Table 4. Comparison of OLS and GWR Model Parameters.

Analysis Model	OLS	GWR
AICc	-81919.767888	-98087.047183
R2	0.508884	0.775181
Adj-R2	0.508862	0.765121

AICc, R^2, and Adi-R^2 can be used to analyze the performance of models. The higher the values of R^2 and Adi-R^2 and the lower the value of AICc, the better the model performance (Li, Zhao and Xu, 2017). A comparison of the parameters of the GWR and OLS models is shown in Table 4. The AICc value of the GWR model is - 98087.047183, which is lower than the OLS model's -81919.767888; the adjusted R^2 is 0.765121, which is higher than the OLS model's 0.508862, indicating that the GWR model performs better. The Std. Residual can be used to determine if there are local problems with the results of the GWR analysis—areas with a standardized residual that is more than 2.5 times the Std. Residual should be investigated. Judging from the visualization of the Std. Residual given by the GWR analysis results (as shown in Fig. 5), there are basically no areas with a Std. Residual greater than 2.5 times the Std. Residual, indicating that the analysis results are reliable.

The GWR analysis shows that there is spatial heterogeneity in the effect of building density on heat health risks, i.e., there are differences in the direction and strength of the effect in different spatial locations. The regression coefficient reflects the effect of building density on heat health risks. The sign of the coefficient indicates the direction of the effect of the independent variable on the dependent variable, and the magnitude of the absolute value of the coefficient indicates the strength of the effect. Table 5 shows that the regression coefficient of building density is positive in each grid, indicating that it contributes to heat health risks. The increase in building density caused by urban development exacerbates the heat health risk. The heat health risk index ranges from 0.011 to 0.335, while the average value of the regression coefficient of building density is 0.278665, indicating that the effect of building density on heat health risk is significant.

Table 5. Regression Relationship between Building Density and Heat Health Risk

	Regression Coefficient			R^2
	Minimum	Maximum	Mean	
BSF	0.003474	2.168746	0.278665	0.775181

From the results of the building density regression coefficient grid (Fig. 6), it can be seen that the impact of building density on heat health risk is generally more significant in unbuilt areas, which is manifested by the fact that the areas with higher regression coefficients (where the impact of building density is higher) are concentrated in the southeast and north of Shenzhen, especially in parts of Dapeng New District and Longhua District, indicating that the impact of building density on heat health risk in these areas is very significant. In contrast, the regression coefficients are lower for built-up areas such as Nanshan District, Bao'an District, Futian District, and Luohu District. These areas were developed and built relatively quickly at an early stage, and the building density has already reached a very high level. Urban construction has a relatively small impact on increasing heat health risks.

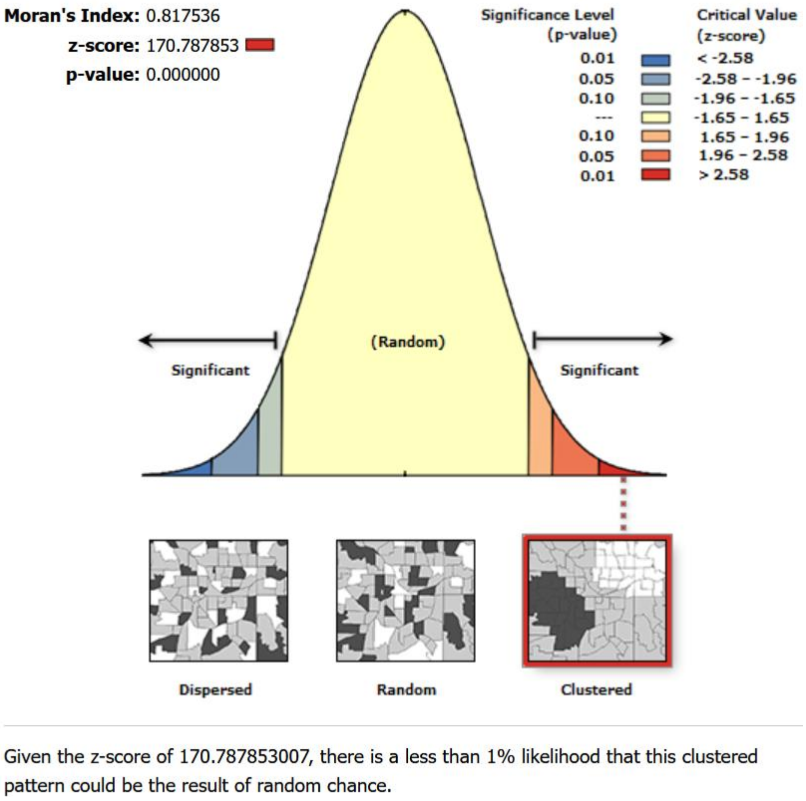

Figure 4. Moran's Index test result.

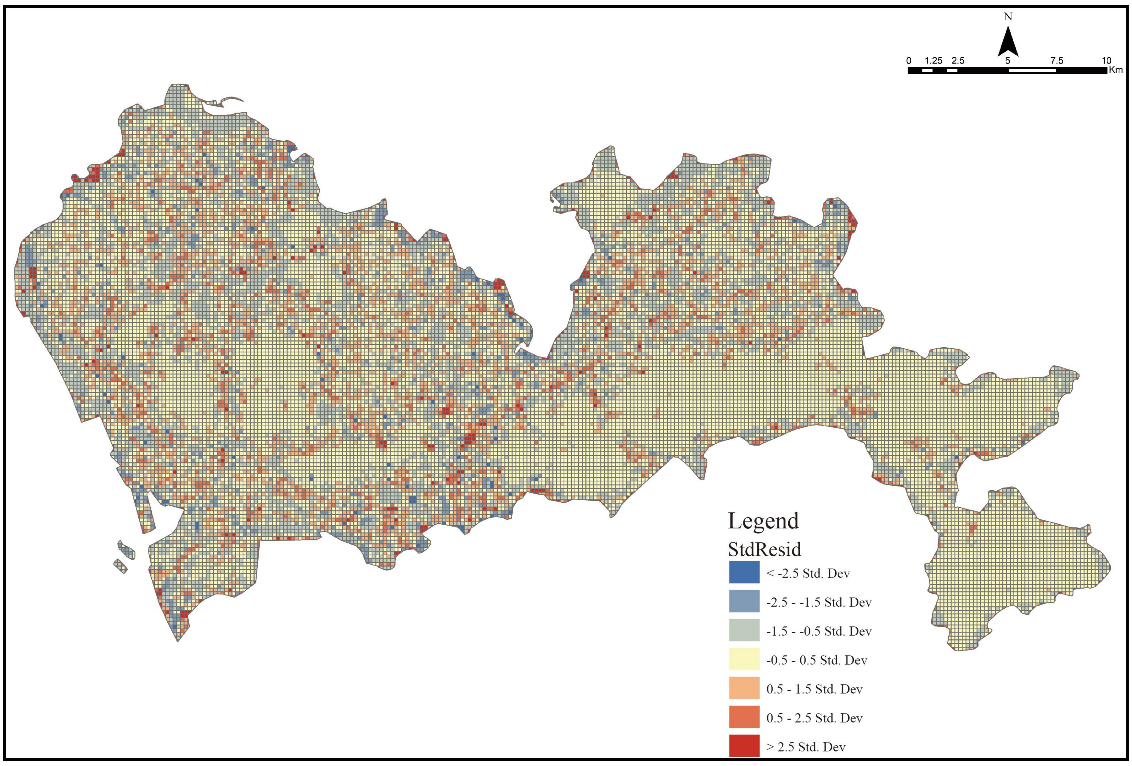

Figure 5. GWR Analysis Std. Residual Visualisation Results of Shenzhen.

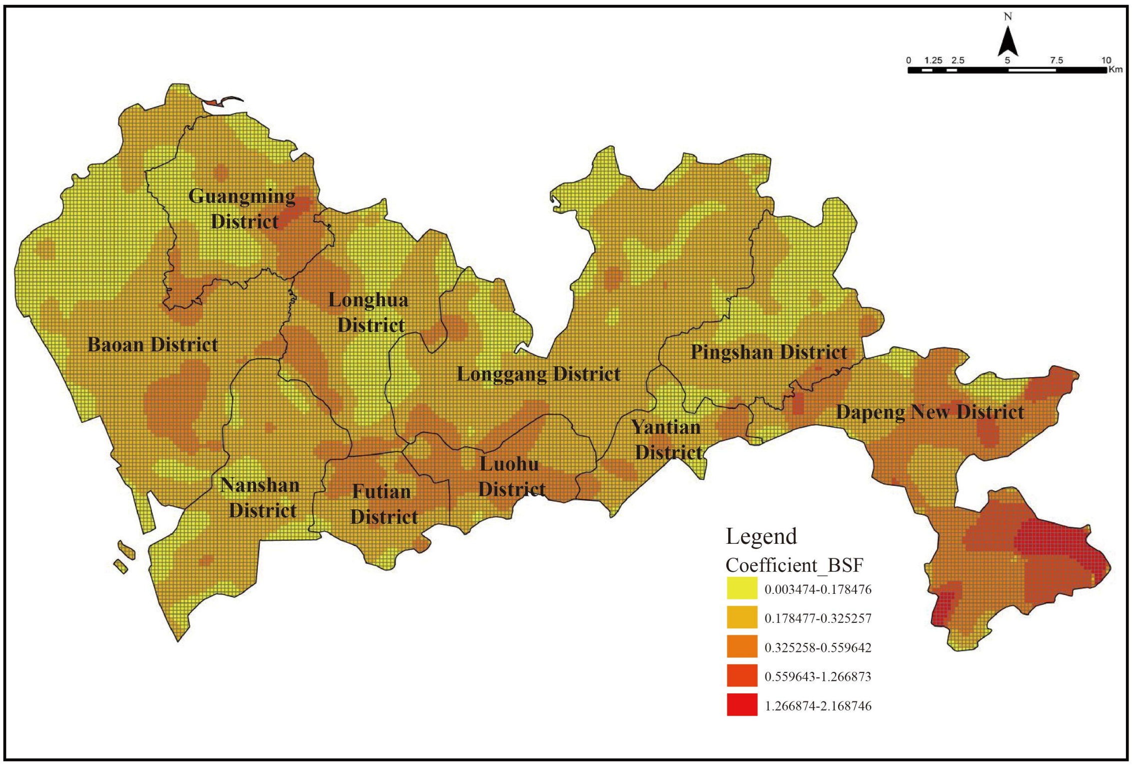

Figure 6. The results of the building density regression coefficient grid

5. Strategy

5.1. Planning stage

There is still a large amount of undeveloped land in outlying urban areas such as Shenzhen's Yantian and Dapeng New Districts. Therefore, during the planning phase, urban planning regulations must be established or amended, and urban master plans, along with detailed plans, should be implemented to accurately define functional zoning and impose restrictions on building density in each area, thereby preventing excessive construction that could intensify heat-related health risks. Promoting a polycentric and multi-level urban layout is essential to avoid single-center, high-density growth and mitigate the strain on the thermal environment. Mitigating heat health concerns in urban environments can be achieved by the strategic design and development of low-density residential zones or satellite cities to encourage people to relocate to these regions.

5.2. Urban construction stage

During urban construction, developers should use highly reflective building materials, solar energy, and green vegetation to cover buildings in Dapeng New District and other uncompleted areas of Shenzhen, increase tree canopies and water bodies, improve blue-green space integrity and connectivity, increase road surface permeability, and reduce high-density low-rise residential areas and open low-lying grasslands. Minimize converting blue-green places, including forests, grasslands, arable land, and water bodies, to construction land to reduce deterioration.

5.3. Urban renewal stage

By the end of 2022, urban villages in Shenzhen will account for more than 40% of the city's total building volume, and the actual resident population will account for about 60% of the city's actual population (China Development Institute (Shenzhen), 2023). During the urban renewal stage, old communities are renovated, and self-built illegal structures are demolished to reduce building density while increasing public space, green areas, water bodies, and infrastructure. In low-density neighborhoods, the demolished building areas can be converted into lawns, community parks, etc., while in high-density neighborhoods, corner plots and vacant lots can be used to create pocket parks and increase the area of blue and green space in the neighborhood.

6. Conclusion

This study constructs Crichton's risk triangle model, integrates multi-source data such as remote sensing image data, selects nine indicators to assess heat health risk in Shenzhen, and uses geographically weighted regression model to explore the effect of building density on heat health risk. It was found that there is significant spatial autocorrelation in heat health risk, and that building density has a significant positive effect on heat health risk. This study further investigates heat health risk mitigation strategies from the perspective of urban planning, providing a foundation and recommendations for Shenzhen to implement heat environment optimization initiatives. Nonetheless, certain limitations persist in the current research. The analysis is confined to the overall status of heat health risks in Shenzhen for 2021; future studies could incorporate data from additional years to examine the spatio-temporal evolution characteristics of these risks. With rapid urban expansion, the influence of heat health risks is progressively extending beyond individual cities into urban agglomerations. Consequently, exploring heat health risk within urban agglomerations represents a critical area for future inquiry, particularly regarding the Guangdong-Hong Kong-Macao Greater Bay Area.

7. References

Anderson, G.B. and Bell, M.L. (2011) ‘Heat waves in the United States: Mortality risk during heat waves and effect modification by heat wave characteristics in 43 U.S. communities’, *Environmental Health Perspectives*, 119(2), pp. 210–218. [online]. Available at: https://doi.org/10.1289/ehp.1002313 (Accessed: 15 August 2024)

Buscail, C., Upegui, E. and Viel, J.-F. (2012) ‘Mapping heatwave health risk at the community level for public health action’, *International Journal of Health Geographics*, 11(1) [online]. Available at: https://doi.org/10.1186/1476-072x-11-38 (Accessed: 15 August 2024)

Che, Y., Li, X., Liu, X., Wang, Y., Liao, W., Zheng, X., ... and Dai, Y. (2024) ‘3D-GloBFP: the first global three-dimensional building footprint dataset’, *Earth System Science Data Discussions*, 2024, pp. 1–28 [online]. Available at: https://doi.org/10.5194/essd-2024-217. (Accessed: 15 August 2024)

Chen, Q., Chen, Q., Chen, Y., et al. (2021) ‘The influence of sky view factor on daytime and nighttime urban land surface temperature in different spatial-temporal scales: A case study of Beijing’, *Remote Sensing*, 13(20), pp. 4117–4117. [online]. Available at: https://doi.org/10.3390/rs13204117 (Accessed: 15 August 2024)

Chen, Z., Yu, B., Yang, C., Zhou, Y., Yao, S., Qian, X., Wang, C., Wu, B. and Wu, J. (2021). An extended time series (2000–2018) of global NPP-VIIRS-like nighttime light data from a cross-sensor calibration.

Earth System Science Data, 13(3), pp.889–906. [online]. Available at: https://doi.org/10.5194/essd-13-889-2021 (Accessed: 15 August 2024)

Dong, W., Liu, Z., Liao, H., Tang, Q., and Li, X. (2014) 'Assessing heat health risk for sustainability in Beijing's urban heat island', *Sustainability*, 6(10), pp. 7334–7357. [online]. Available at: https://doi.org/10.3390/su6107334 (Accessed: 15 August 2024)

Field, B.C., Barros, R.V., Dokken, J.D., et al. (2014) Climate Change 2014: Impacts, Adaptation, and Vulnerability. Cambridge: Cambridge University Press [online]. Available at: https://doi.org/10.1017/CBO9781107415379 (Accessed: 24 August 2024)

Fotheringham, A.S., Charlton, M.E. and Brunsdon, C. (1998) 'Geographically weighted regression: A natural evolution of the expansion method for spatial data analysis', *Environment and Planning A: Economy and Space*, 30(11), pp. 1905–1927. Available at: https://doi.org/10.1068/a301905 (Accessed: 15 August 2024)

Gong, P., Liu, H., Zhang, M., et al. (2020) 'Annual maps of global artificial impervious area (GAIA) between 1985 and 2018', *Remote Sensing of Environment*, 236, p. 111510. [online]. Available at: https://doi.org/10.1016/j.rse.2019.111510 (Accessed: 15 August 2024)

Guo, A., Zhang, Y., Zhu, L., et al. (2020) 'Impact of urban morphology and landscape characteristics on spatiotemporal heterogeneity of land surface temperature', Sustainable Cities and Society, 63, pp. 102443–102443. [online]. Available at: https://doi.org/10.1016/j.scs.2020.102443 (Accessed: 15 August 2024)

Hien, W.N., Jusuf, S.K., Samsudin, R. and Jiang, S.W. (2019) 'Modeling the impact of urban planning on climate in high-density cities: A case study of the Singapore CBD', *Urban Planning Journal*, (04), p. 124.

Hu, K., Zhang, Y., Xu, Z., Li, B., and Jin, L. (2017) 'Spatially explicit mapping of heat health risk utilizing environmental and socioeconomic data', *Environmental Science & Technology*, 51(3), pp. 1498–1507. [online]. Available at: https://doi.org/10.1021/acs.est.6b04355 (Accessed: 15 August 2024)

Intergovernmental Panel on Climate Change (2021) *Climate Change 2021: The Physical Science Basis. Contribution of Working Group I to the Sixth Assessment Report of the Intergovernmental Panel on Climate Change*. Cambridge: Cambridge University Press.

Johnson, D.P., Stanforth, A., Lulla, V. and Luber, G. (2012). Developing an applied extreme heat vulnerability index utilizing socioeconomic and environmental data. *Applied Geography*, 35(1-2), pp.23–31. [online]. Available at: https://doi.org/10.1016/j.apgeog.2012.04.006 (Accessed: 15 August 2024)

Li, C., Zhao, J. and Xu, Y. (2017) 'Examining spatiotemporally varying effects of urban expansion and the underlying driving factors', *Sustainable Cities and Society*, 28, pp. 307–320. [online] Available at: https://doi.org/10.1016/j.scs.2016.10.005 (Accessed: 15 August 2024)

Lin, P., Li, X., Yuan, X., Liu, Q. and Li, Z. (2017) 'Effects of urban planning indicators on urban heat island: a case study of pocket parks in high-rise high-density environment', *Landscape and Urban Planning*, 168, pp. 48–60. [online]. Available at: https://doi.org/10.1016/j.landurbplan.2017.09.024 (Accessed: 15 August 2024)

Liu, J., Chen, T., & Wang, L. (2022) 'Identification, assessment, and urban design interventions for heat health risks in high-density cities from a climate change perspective: A case study of Macau', *Urban*

Planning International, pp. 1-14. [online]. Available at: https://doi.org/10.19830/j.upi.2022.135 (Accessed: 15 August 2024)

Liu, H., He, Y., Tang, J., et al. (2019) 'Seasonal variation of the spatially non-stationary association between land surface temperature and urban landscape', Remote Sensing, 11(9), pp. 1016–1016. [online]. Available at: https://doi.org/10.3390/rs11091016 (Accessed: 15 August 2024)

Liu, Y., Wu, K., Li, X., et al. (2021) 'Complexity of the relationship between 2D/3D urban morphology and the land surface temperature: a multiscale perspective', Environmental Science and Pollution Research, 28(47), pp. 66804–66818. [online]. Available at: https://doi.org/10.1007/s11356-021-15177-7 (Accessed: 15 August 2024)

Lu, B., Ge, Y., Qin, K., et al. (2020) 'A review of geographically weighted regression analysis techniques', *Journal of Wuhan University (Information Science Edition)*, 45(09), pp. 1356–1366. [online]. Available at: 10.13203/j.whugis20190346.(Accessed: 15 August 2024)

Lu, Y., Chen, Y., Liu, S., and Xu, Q. (2021) 'Investigating the spatiotemporal non-stationary relationships between urban spatial form and land surface temperature: A case study of Wuhan, China', *Sustainable Cities and Society*, 72, pp. 103070–103070. [online]. Available at: https://doi.org/10.1016/j.scs.2021.103070 (Accessed: 15 August 2024)

Moran, P.A.P. (1948) 'The interpretation of statistical maps', *Journal of the Royal Statistical Society Series B: Statistical Methodology*, 10(2), pp. 243–251. [online]. Available at: https://doi.org/10.1111/j.2517-6161.1948.tb00012.x (Accessed: 15 August 2024)

Moran, P.A.P. (1950) 'Notes on continuous stochastic phenomena', *Biometrika*, 37(1–2), pp. 17–23. [online]. Available at: https://doi.org/10.1093/biomet/37.1-2.17 (Accessed: 15 August 2024)

Nieves, J.J., Sorichetta, A., Linard, C., Bondarenko, M., Steele, J.E., Stevens, F.R., Gaughan, A.E., Carioli, A., Clarke, D.J., Esch, T., and Tatem, A.J. (2020) 'Annually modelling built-settlements between remotely-sensed observations using relative changes in subnational populations and lights at night', *Computers, Environment and Urban Systems*, 80, p. 101444. Available at: https://doi.org/10.1016/j.compenvurbsys.2019.101444 (Accessed: 15 August 2024)

Nieves, J.J., Bondarenko, M., Sorichetta, A., Steele, J.E., Kerr, D., Carioli, A., Stevens, F.R., Gaughan, A.E., and Tatem, A.J. (2020) 'Predicting near-future built-settlement expansion using relative changes in small area populations', *Remote Sensing*, 12, p. 1545. Available at: https://doi.org/10.3390/rs12101545 (Accessed: 15 August 2024)

Pezzulo, C., Hornby, G., Sorichetta, A., et al. (2017) 'Sub-national mapping of population pyramids and dependency ratios in Africa and Asia', *Scientific Data*, 4, p. 170089. [online]. Available at: https://doi.org/10.1038/sdata.2017.89 (Accessed: 15 August 2024)

Sun, Z. (2020) 'Impact of morphological elements in high-density urban areas on thermal environment: A case study of the area within the Fifth Ring Road in Beijing', *Journal of Ecology and Environment*, (10), pp. 2020–2027. [online]. Available at: https://doi.org/10.16258/j.cnki.1674-5906.2020.10.012 (Accessed: 15 August 2024)

Wang, M., Liang, S., Zeng, Y., Li, X., Yu, L., and Cheng, J. (2019) 'A practical single-channel algorithm for land surface temperature retrieval: Application to Landsat series data', *Journal of Geophysical Research: Atmospheres*, 124(1), pp. 299–316. [online]. Available at: https://doi.org/10.1029/2018jd029330 (Accessed: 15 August 2024)

WorldPop (2018) *Global High Resolution Population Denominators Project - Funded by The Bill and Melinda Gates Foundation (OPP1134076)*. School of Geography and Environmental Science, University of Southampton; Department of Geography and Geosciences, University of Louisville; Departement de Geographie, Universite de Namur, and Center for International Earth Science Information Network (CIESIN), Columbia University. Available at: https://dx.doi.org/10.5258/SOTON/WP00675 (Accessed: 15 August 2024)

WorldPop (2018) *Global High Resolution Population Denominators Project - Funded by The Bill and Melinda Gates Foundation (OPP1134076)*. School of Geography and Environmental Science, University of Southampton; Department of Geography and Geosciences, University of Louisville; Departement de Geographie, Universite de Namur, and Center for International Earth Science Information Network (CIESIN), Columbia University. Available at: https://dx.doi.org/10.5258/SOTON/WP00646 (Accessed: 15 August 2024)

Yuan, Q., Meng, J. and Leng, H. (2021) 'Urban spatial impacts and planning interventions of health risks from climate change', *Urban Planning*, 45(03), pp. 71–80. [online]. Available at: https://doi.org/10.11819/cpr20210309a (Accessed: 15 August 2024)

Zhao, L., Oleson, K., Bou-Zeid, E., Frolking, S., Krayenhoff, E.S., Bray, A., Zhu, Q., Gao, Z. and Liu, Y. (2021) 'Global multi-model projections of local urban climates', *Nature Climate Change* [Preprint]. [online]. Available at: https://doi.org/10.1038/s41558-020-00958-8 (Accessed: 15 August 2024)

Zhao, Y., Wang, N., Liu, Y., et al. (2021) 'Quantification of ecosystem services supply-demand and the impact of demographic change on cultural services in Shenzhen, China', *Journal of Environmental Management*, 304, pp. 114280–114280. [online]. Available at: https://doi.org/10.1016/j.jenvman.2021.114280 (Accessed: 15 August 2024)